Maintenance and Rehabilitation

# Image-based 3D reconstruction using traditional and mobile-phone data-sets for road pavement distress analysis

*Ronald Roberts, Laura Inzerillo, Gaetano Di Mino*
*University of Palermo*

Abstract

The issue of road networks being in deplorable conditions is one that is widespread globally. One of the main precursors for this is that when preparing maintenance management systems, many road agencies rely on data which is often outdated or inaccurate. This is due in many cases to insufficient budgets which are unable to adequately address both maintenance and rehabilitation. It is therefore critical that road agencies have better tools at their disposal to help combat these issues. One of the possible techniques that have been identified is the use of structure from motion techniques to adequately identify road pavement distresses. This paper advances previous work in this area and explores the accuracy of using mobile phones to collect the imagery as opposed to traditional methods relying on professional cameras and equipment. This would provide a lower cost and readily available alternative for practitioners. The techniques have been applied on a distressed pavement in Palermo, Italy using data-sets from a mobile phone and a professional camera to analyse the quality and adequacy of using data-sets from the mobile phone. The results indicate that the mobile phone data-sets can adequately utilize the techniques and therefore this incites the possibility of integrating mobile integrations with the technology specifically focused on pavement management systems.

This paper was first published in 2020 in version 1.0 of the proceedings of the 7th E&E Congress. This second edition (version 1.1.) of the proceedings is published in June 2021. The content of this paper has not changed, but the author(s) may have provided additional information in the form of an annex.

# 4. INTRODUCTION

## 4.1 State of pavement distress detection worldwide

Globally there are substantial difficulties faced by Road Authorities when carrying out required Road Maintenance and Rehabilitation activities. This is due to decreased available program budgets globally [1,2] which in many instances leads to inefficient maintenance scheduling and development. These programs are typically developed within a Pavement Management System (PMS) [3] which is set up to ensure that the available funds are utilized in the best possible manner for the required activities. However, the PMS is data-dependent and for it to function properly and optimize road maintenance management, accurate road condition data is required. The availability of this information allows for financial savings as more preventative maintenance can be done extending the pavement's life cycle [4] whilst avoiding excessive corrective maintenance.
Obtaining road condition data can be expensive as the most accurate methods are usually very expensive and as a result in many instances, road condition data is collected by manual methods [5]. However, data from these methods are subjective and can lead to the development of poor maintenance strategies. To this end, there has been a lot of research into developing new methods and technologies for the purpose of road pavement distress detection [6], which can, in turn, be utilized within the asset management system. The two largest areas of development have been using lasers and imagery or a combination of the two. Of the two, laser-based systems have shown to be very accurate and reliable but these benefits come at a higher cost which in most cases cannot be borne by Road agencies with budget deficiencies. Conversely, systems and techniques based on imagery have shown continual increases in their accuracies. Whilst these systems are not as accurate as laser-based ones, they can still provide reliable data for road agencies at a lesser cost.

## 4.2 The utilization of a low-cost pavement distress detection and analysis technique

This study focuses on a low-cost detection technique that can help solve road condition data acquisition issues. The study applies an image-based technique, namely the use of Structure-from-Motion which is a photogrammetric technique that generates 3D models of objects using simple 2D imagery [7]. This technique has been utilized recently for the analysis of pavement distresses [8] with accurate and reliable 3D models of distresses being developed which can be used within an asset management system. It relies on imagery of a particular object and therefore the device used to obtain the images is very important.
Mobile phones have been considered as possibilities to generate datasets for this technique in other sectors given their availability and cost [9]. This is due to the ever-increasing quality and performances of smartphone cameras which have shown accuracies close to high-cost professional cameras [10]. Given this, it is necessary to determine if imagery from typical smartphones can adequately conduct the Image-based modelling necessary for pavement distress applications. As a result, this study was developed to answer the question of whether cameras from a range of different smartphones can adequately be used to reconstruct pavement distresses. The study considers the use of five different smartphones to generate 3D pavement distresses models and compares these models to a base model using a professional camera to determine the accuracy and validate the replicability of the process.

# 5. STATE OF THE ART – THE USE OF 3D MODELLING

## 5.1. Background of image-based distress detection methods

There have been numerous applications of image-based distress detection techniques for the purpose of detecting and analysing pavement distresses. Typically these methods involve the collection of a large set of images of the pavement and then subsequent analysis of these images. There have several algorithms developed for the purpose of detecting distresses within images [12,13].
Within the scope of image-based techniques, there has also been the development of stereoscopic techniques. This includes the use of Photogrammetry and Structure-from-Motion (SfM) techniques. These methods utilize images to reconstruct three-dimensional models of the distress. The techniques themselves are not new and there have been previous attempts to incorporate them into pavement distress applications [14–17]. However, criticisms have been made which include limitations with respect to accuracy, computational requirements and software availability. However, these accuracies have improved significantly with improvements in software and computational resources [18]. This has led to recent work utilizing the improved workflows for the replication of pavement distresses. However there is still substantial work to be done in this area to determine the practicality of using these techniques in industry including testing of the techniques with mobile phones for pavement distress applications. This aim of this study is to validate the use of the techniques considering multiple mobile phones.

## 5.2. Structure-from-Motion and 3D Modelling

Structure-from-Motion (SfM) is a photogrammetric technique, which enables a user to create a 3D model utilizing overlapping 2D imagery. It is a low-cost technique which offers high resolution in reconstructing an object in three

dimensions [19]. For a typical survey, imagery is captured around an object with an overlap of 70-80%. Following this, the imagery is processed through a standardised SfM pipeline, which carries out image alignment followed by reconstructing the object's position in space and then finally the generation of a 3D model. This is done with the use of a bundle adjustment procedure using common features that were automatically extracted from the overlapped images [20]. The identification of common points allows the algorithm to detect where the point exists in three dimensions. This is done exploiting SfM software wherein the pipeline is built in. In figure 1 below an example of how the images are captured is shown wherein the blue rectangles represent the location of the camera during the survey of a distressed pavement section. The developed 3D model is also shown which was generated utilizing the modelling software, Agisoft PhotoScan.

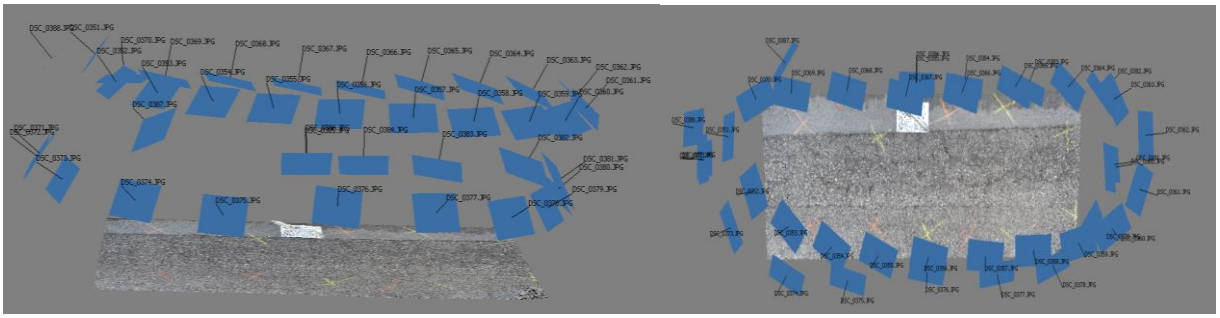

**Figure 1: Example dataset during a survey of a distressed pavement section**

Once the 3D model of the pavement distress is generated, the models can be analysed and measured to determine the exact distress type and critically, the severity level. The method allows a user to extract critical metric information such as the length and width of a distress as well as the area covered by the distress, which are representative of the metrics used by the industry to classify the distress [8]. Using this information, road agencies can have up to date information on the road conditions at specific points and it is possible to monitor large sections using drones equipped with cameras, which would allow a model of a large section to be created. For specific distresses on a road, an engineer can carry out a quick survey of the distress or the distressed section and generate the model for analysis and interpretation. This pipeline is depicted in figure 2.

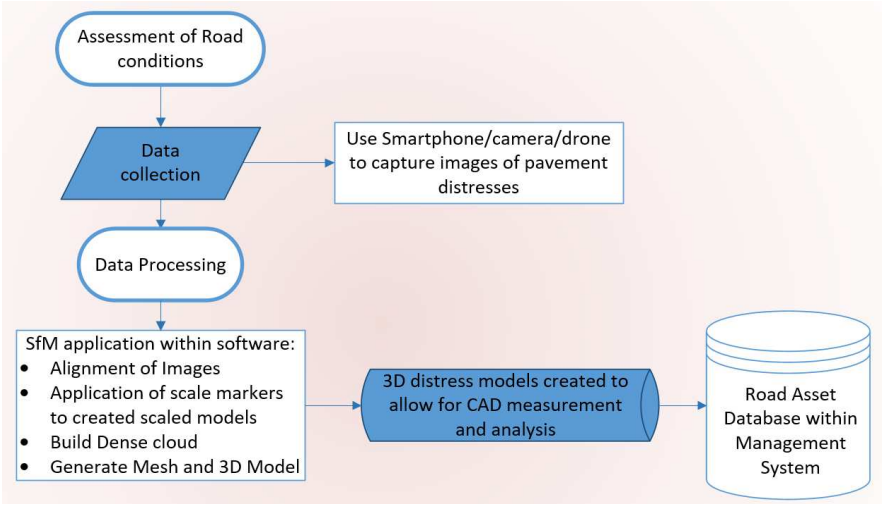


**Figure 2: Pipeline for utilizing the SfM technique for Pavement distress applications**

### 5.3. The objective of Study – the analysis of practical applications of SfM pipelines with common smartphones

Whilst the techniques have been utilized with mobile phones before, the research on this has been focused on the areas of cultural heritage and architecture where the photogrammetric techniques have generally been used [21]. For the use of these techniques in practical road applications, the accuracies of different phones are important. This is due to the large variety of mobile phones available on the market. These phones vary by brand and cost. The question, therefore, arises as to the impact a different phone will have on the production of the 3D models and the distress survey. Given the large market range, this study aimed to carry out distress analysis with five different phones available to the research team, which were: Samsung Galaxy S9, iPhone XR, Huawei P20 Pro, Google Pixel 2XL and Xiaomi Mi A1. These phones have different technical specifications and costs but provide a good overview of the phones available.

The aim of this was not to declare a winner among these phones or a preference amongst brands but instead to determine if the methodology could work on a range of different devices and still produce adequate models that

could be used in pavement distress analysis. This is important to determine the reliability and replicability of using this methodology in real-world conditions in road applications wherein there is no consensus phone brand choice and users will have to utilize the techniques with their available phones. The models generated were compared to models generated by a professional camera so as to have a control point in the study.

## 6. METHODOLOGY - EXPERIMENTAL SETUP

### 6.1. Devices

For the purpose of this study, five smartphones available within the research team were utilized and the camera specifications of these devices are shown in Table 1. There are variations amongst the camera resolutions and image size which allows for a greater sample for the study.

**Table 1. Device Specifications**

| Device | Nikon D5200 | Huawei P20 Pro | Samsung Galaxy S9 | iPhone XR | Google Pixel 2XL | Xiaomi Mi A1 |
|---|---|---|---|---|---|---|
| Camera resolution [Megapixel] | 24 | 40 | 12 | 12 | 12 | 12 |
| Image Size [pixel] | 6000 x 4000 | 7152 x 5368 | 4032 x 3024 | 4032 x 3024 | 4032 x 3024 | 3968 x 2976 |

### 6.2. Procedure

Once the devices were chosen, the following steps were carried out for the study:

1. Data collection – Using the professional camera and the phones, photographic datasets were acquired of two distress types: a cracked pavement section and a pothole on an urban asphaltic pavement surface within the city of Palermo, Italy. These were chosen as these represent two common distress types and cracking is the most dominant type of distress in the region [11].
2. The photos were taken in a sequence on the pavement, with coded markers on the road surface used for scaling of the models. Images were taken ensuring there was an angle between each shot of 5 to 10 degrees and an overlap of 80%. The surveys were done within the same time period during the day with the same clear and bright light conditions. Each survey per device took approximately 10 minutes and they were carried out consecutively to allow for comparability.
3. Data Processing – The images were then imported into the SfM software, Agisoft PhotoScan wherein the previously explained SfM pipeline was carried out to generate textured 3D models of each distress per device.
4. Estimation of reliability – The models generated by the phones were then compared to the models generated by the professional camera. This was done utilizing the free open source software CloudCompare which is used for the analysis of point clouds and models. Within this software, the models were aligned and compared for each distress and for each device against the model created by the camera. An example of the model alignment of the cracked section in the CloudCompare environment is shown below in figure 3.

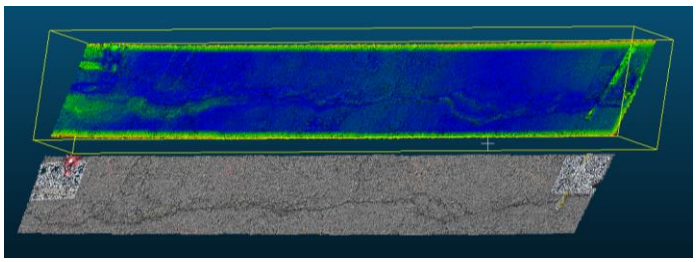

**Figure 3: Alignment and comparison of models in CloudCompare**

5. Analysis of comparisons of models – Analysis of the model comparisons were then made to identify key findings and recommendations for the future integration of the modelling techniques.

## 7. RESULTS AND DISCUSSIONS

### 7.1. Cracked Pavement section

The cracked section identified for the study is showcased in Figure 4, wherein an image during the data acquisition using the professional camera is shown as well as one of the datasets and models generated during the study. The cracked section exhibits longitudinal and transverse cracking, which are the most dominant type of distress on Italian urban roadways [11].

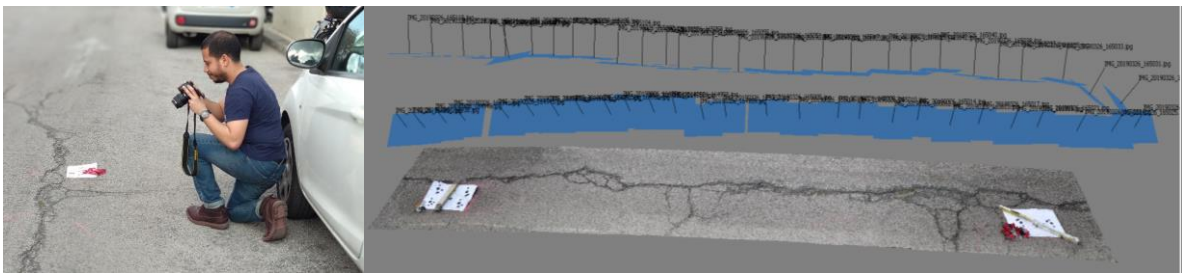

**Figure 4: Cracked pavement section used for the study**

For the surveys carried out on this section survey specifications for each device are depicted in Table 2 below.

**Table 2. Survey specifications for cracked section**

| Device | Nikon D5200 | Huawei P20 Pro | Samsung Galaxy S9 | iPhone XR | Google Pixel 2XL | Xiaomi Mi A1 |
|---|---|---|---|---|---|---|
| Distance from the pavement [mm] | ~100 | ~100 | ~100 | ~100 | ~100 | ~100 |
| Number of photos taken [-] | 59 | 56 | 45 | 57 | 69 | 65 |
| Ground Sample Distance(GSD) [mm/pixel] | 0.012 | 0.0250 | 0.0275 | 0.0294 | 0.0282 | 0.0321 |
| Mesh faces created in SfM software[-] | 8,295,756 | 3,438,510 | 2,453,349 | 1,631,836 | 2,710,814 | 1,467,604 |

In Table 2, there is a variation in the number of photos taken. This is deliberate so as to create a range of situations likely to occur in real-world scenarios with different users. The distance of the device from the pavement was however kept consistent to allow for comparability between models. The table also details the Ground Sample Distance (GSD) of the models created. The GSD is a value that denotes the distance between two sequential pixels centres on an image as measured on the ground. Its value is representative of the smallest observable detail on an image. [22]. For the resulting 3D models, the tiniest visible and measurable details are 2 to 3 times the GSD value [23]. The lower the GSD value is, the more details can be extracted from your model. Therefore, a lower GSD value gives the user a larger scope of metric analysis possibilities. This is critical as it means that for a model to effectively measure 1mm of detail, the GSD has to be approximately 0.33mm. This condition was met in all of the models created by each device and this means that each model can measure with an accuracy at least of 1mm which would be sufficient for extracting details of the distress and classifying their severity based on the typical severity classifications by industry manuals [24]. It should also be noted that the GSD of the camera model is the highest and this is expected, as the camera resolution is the highest of all the devices used and this is why it was chosen as the control device.

The variable, Mesh faces, also describe the level of details with the camera model clearly having a higher value and therefore having more intricate details displayed. There is a variation of this value but its value is hard to decipher and thus it is more important to visually inspect the models created which is done within the subsequent section.

### 7.2. Comparisons of models of Cracked section

The models generated using the 3D modelling techniques display texture and details of the actual object under investigation. Figure 5 displays the model produced by the camera where the top image displays the textured 3D model and the bottom displays the dense cloud which visualizes the models' intricate details, roughness and shape on the surface without the colour. In the same way, Models from smartphones are displayed in Figure 6.

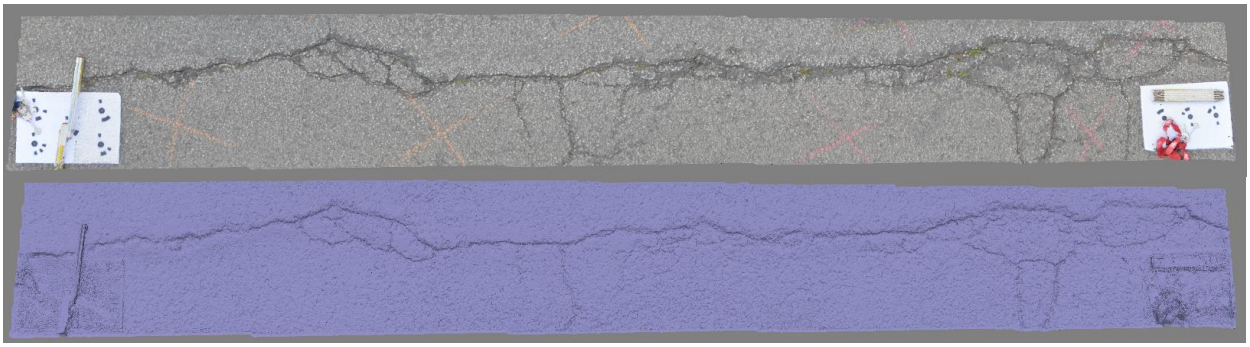

**Figure 5: Model produced by Nikon camera**

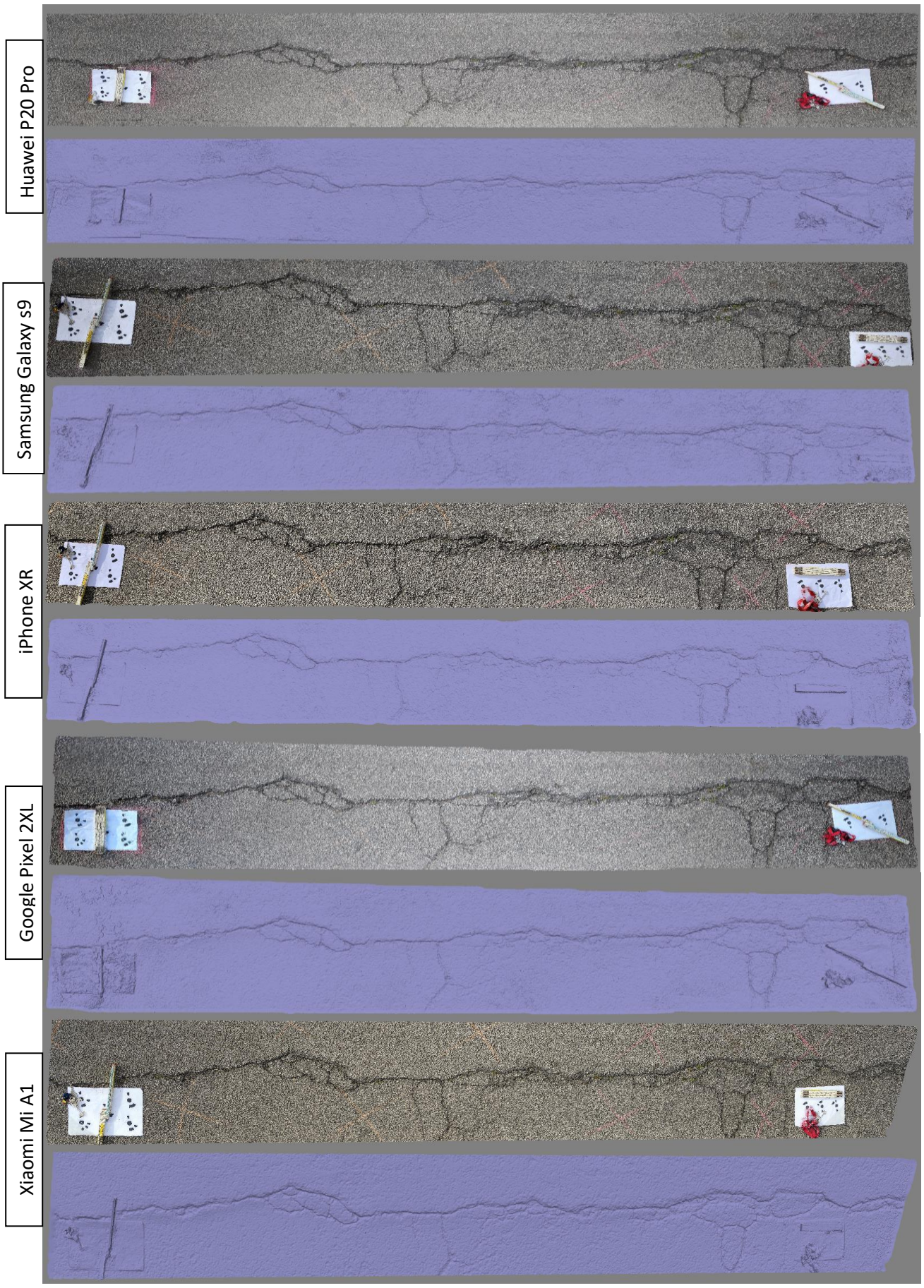


**Figure 6: Models produced by phones**

Each of the models produced appear to visually offer a clear detailing of the cracks on the section. There appears to be colour differences with some of the models produced by the phones. This colour variation can be attributed to the differences in the internal parameters and makeup of the phones and their camera sensors. However, the colour is not important to the determination of the severity of the distress which is critical for a practitioner. Generally, however, the details can be adequately inspected and on this basis, all of the models satisfy this criterion which is essential for the performance during a road survey. However, this represents only a visual inspection and from this, no metric comparisons can be ascertained. To carry out the metric comparisons the models were aligned and compared within the CloudCompare software to have a metric understanding of the differences.

Within CloudCompare, models are compared using a metric called C2C absolute distance which measures distance variations between models. These variations are shown in Figure 8 for each model along with their related histogram distributions. The C2C distance is measured in metres (m). The variations are colour coded from blue to red where blue represents lower deviations and the red represents higher deviations as depicted in the histograms.

For each model, the variations are different. The points on the model where there is the most variation are along the crack's length. Some of the models have fewer variations than others but what is critical is that all of the actual variations are in the range of less than 0.0018m (1.8mm). Given such a low deviation, it signifies that there would be no impact on classifying severity regardless of the phone used for this type of distress as the difference would not change the severity classification. For a more critical examination of the differences, a Weibull distribution was applied to the measured differences. The Weibull distribution is a continuous probability distribution and it was applied as it is typically used to determine the accuracies of structure-from-motion models [26]. This was done within CloudCompare. An example of the application of this distribution plot is shown in figure 7, which validates the use of this distribution as the figure shows how closely the data aligns with the Weibull distribution plot.

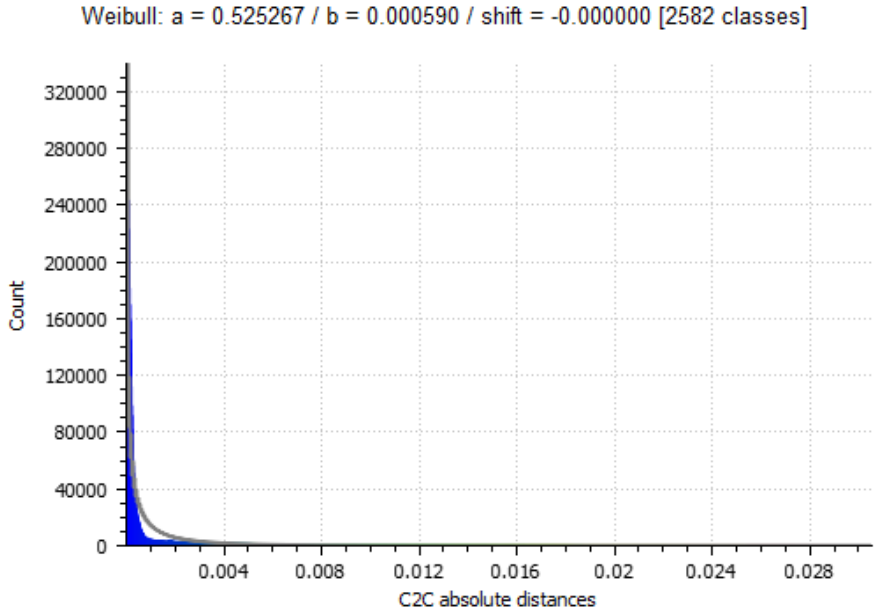


**Figure 7: Weibull distribution applied to the measured differences between models**

The two important resulting parameters from this distribution are the Weibull shape and scale parameters. These are denoted as a, and b, within the software. These parameters from each model are shown in Table 3. The scale parameter indicates that 63.2 percentile of the distribution will fail before reaching this point [25]. Considering the values in the table this signifies that for all of the models this value is less than 0.001m (1mm). Therefore, the difference is negligible considering the metric requirements to determine severity. For the shape parameter, if the value is less than 1, then the majority of values likely occur early in the distribution. This is the case for nearly all models, with the exception of two, but given the fact that the scale values are below 1mm, this can be considered a satisfactory result and the technique can be considered as validated for this type of distress.

**Table 3. Weibull parameters observed from each model comparison for the cracked section**

| | **Weibull parameters** | |
|---|---|---|
| **Phone** | **Shape (a)** | **Scale (b)** |
| Huawei P20 Pro | 1.417948 | 0.000854 |
| Samsung Galaxy s9 | 0.962864 | 0.000688 |
| iPhone XR | 0.61105 | 0.000558 |
| Google Pixel 2XL | 1.374845 | 0.000720 |
| Xiaomi Mi A1 | 0.525267 | 0.000590 |

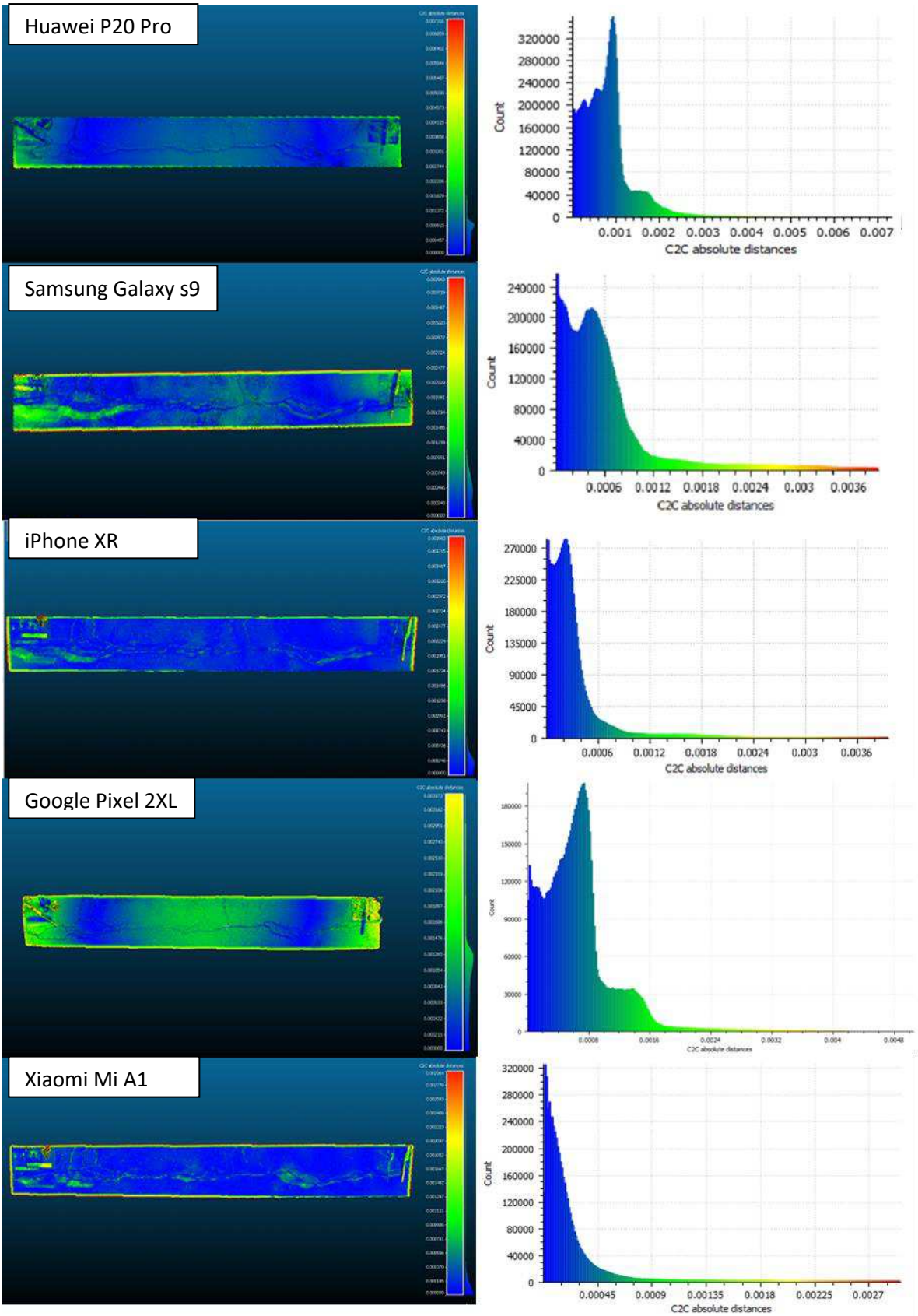


**Figure 8: Comparisons of models of cracked sections**

### 7.3. Pothole

The pothole identified for the study is showcased in Figure 9, wherein an image during the data acquisition using the professional camera is shown as well as one of the datasets and models generated during the study.

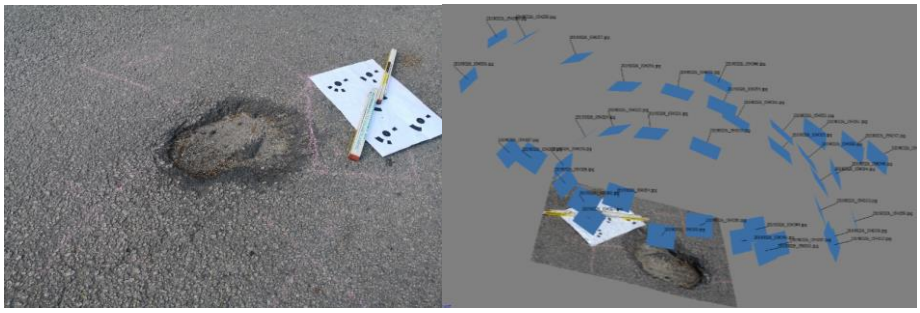

**Figure 9: Pothole used for the study**

For the surveys carried out on this section survey specifications are depicted in Table 4 below.

**Table 4. Survey specifications for Pothole**

| Device | Nikon D5200 | Huawei P20 Pro | Samsung Galaxy S9 | iPhone XR | Google Pixel 2XL | Xiaomi Mi A1 |
|---|---|---|---|---|---|---|
| Distance from the pavement [mm] | ~100 | ~100 | ~100 | ~100 | ~100 | ~100 |
| Number of photos taken [-] | 23 | 44 | 38 | 29 | 30 | 30 |
| GSD [mm/pixel] | 0.0107 | 0.0257 | 0.0215 | 0.0198 | 0.0209 | 0.0252 |
| Mesh faces created in SfM software[-] | 1,740,857 | 782,309 | 1,201,262 | 1,337,492 | 446,207 | 397,593 |

In Table 4, it is noted that again there is a variation in the number of photos taken. This is to serve the same purpose as previously described to generate a range of situations, which are likely to occur in real-world scenarios with different users. The GSD values of each model in Table 4 are also lower than 0.33mm indicating as well that each model can measure to at least an accuracy of 1mm which would be sufficient for extracting details of the pothole distress and classifying their severity. The GSD of the camera model is again the lowest and therefore as expected would offer the highest resolution and therefore is an adequate comparison model for the analysis.
Concerning the variable, Mesh faces, the camera model again clearly has a higher value and therefore is more intricately detailed as expected.

### 7.4. Comparison of Models of the Pothole pavement distress

Using the same methodology as done with the cracked section, models were produced of the pothole distress. These models also display texture and details of the pothole under investigation. The first model displayed is the one produced by the camera and in Figure 10 wherein the image of the left displays the textured 3D model and the right image displays the dense cloud, which allows a user to see the intricate details, roughness and shape on the model's surface without the colour.

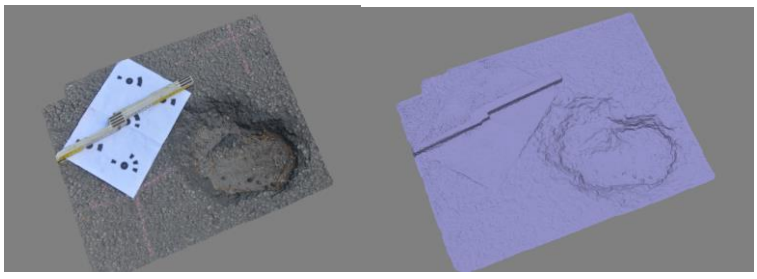

**Figure 10: Model produced by Nikon camera**

The same model development was done for the phones and these textured models and dense clouds are displayed in Figure 11.

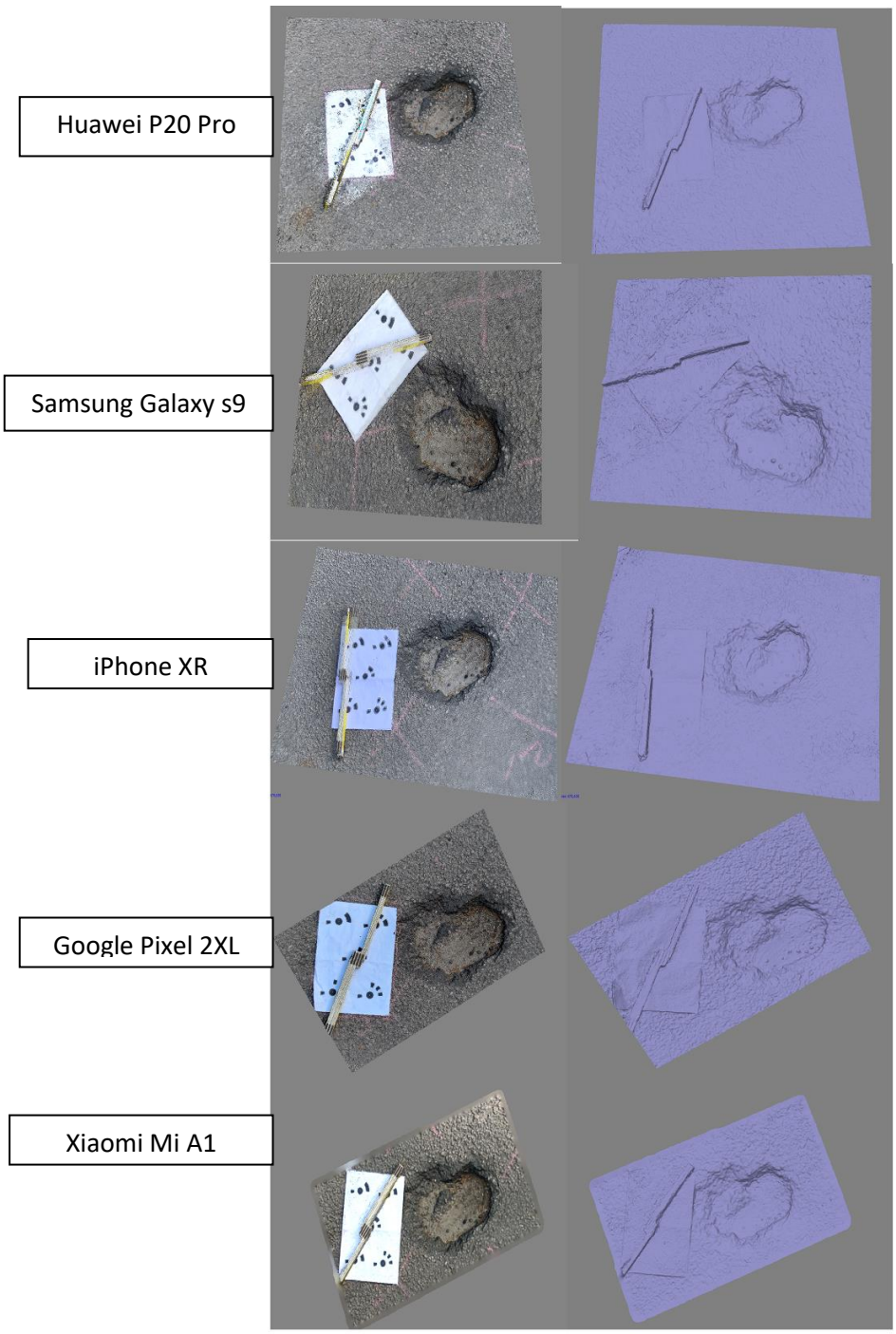


**Figure 10: Models produced by phones**

In Figure 10 above it appears that all of the models produced by the phones appear to visually offer a clear detailing of the pothole and its detailing. Once more, there are differences in the colour of some of the models produced by the phones. The same reasons for this colour variation would apply given the differences in the internal parameters and makeup of the phones and their camera sensors. For this distress type, these models show that the details can be also be adequately inspected and on this basis, all of the models satisfy this criterion.

For the metric analysis, the models were aligned and compared within the CloudCompare software to have a metric understanding of the differences.

The same metric of C2C absolute distance was also used for the evaluation. These variations are shown in Figure 12 for each model along with a histogram distribution of all the variations between the models. The C2C distance is once again measured in metres (m) in Figure 12.

For each model, the variations are different with the points on the model of most variation being on the interior of the pothole at the sides and along its depth. Variations were also seen at the edges of the pavement section and this is due to the differences in the sizes of the patch utilized for each model. Some of the phone models have fewer variations than others but what is critical is that all of the actual variations are in the range of less than 0.0016m,

which is equivalent to 1.6mm. Given such a low deviation, this, therefore, means that there would be no impact on the classification of the pothole's severity regardless of the phone used for this type of distress.

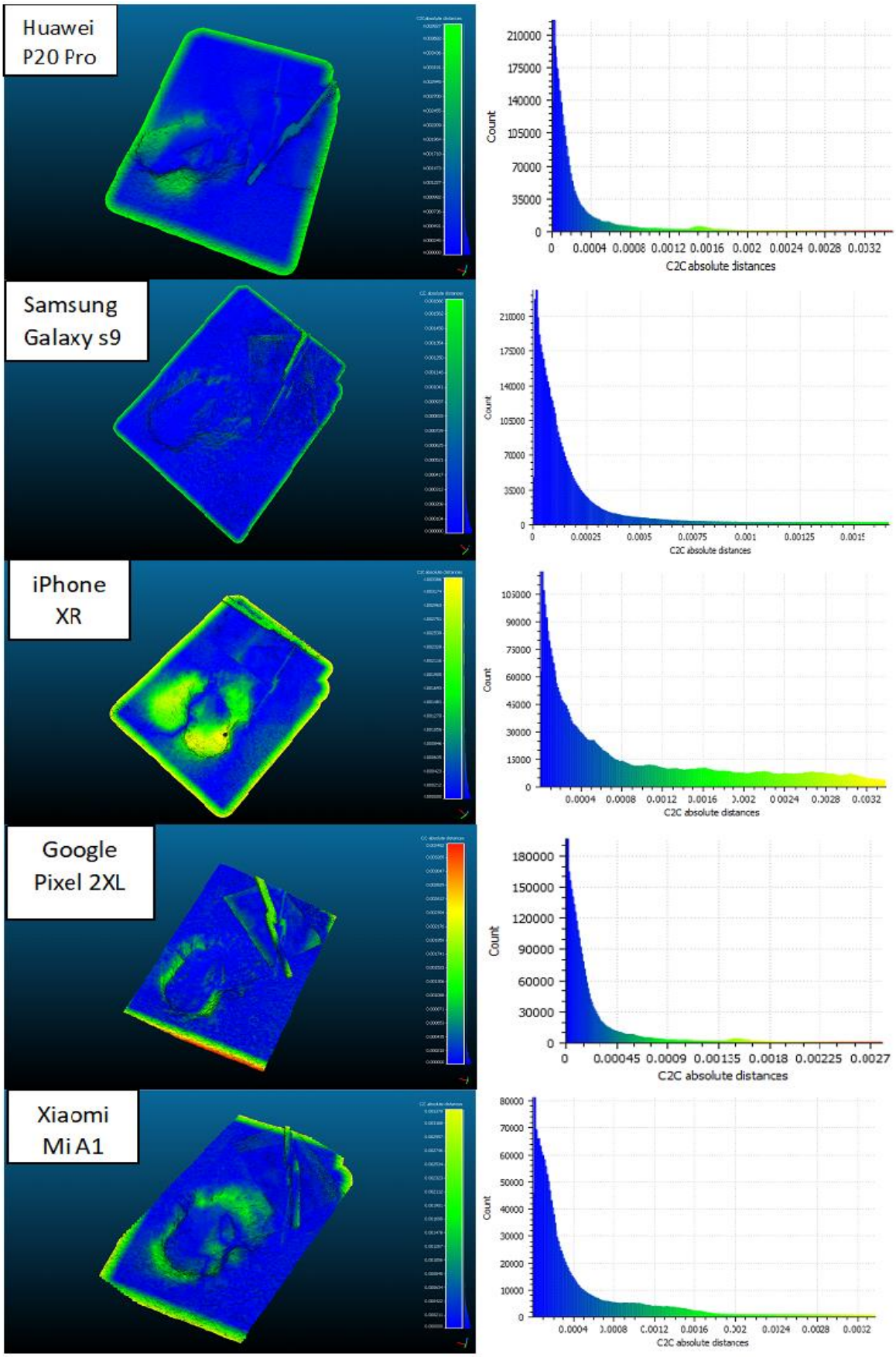


**Figure 12: Comparisons of models of pothole**

As was done with the models for the cracked section, a Weibull distribution computation was applied for the pothole models. The results from these plots are given in Table 5 below and show the scale and shape parameters. Considering the values in the table, similar to the models from the cracked section the scale factors for each model are all less than 0.001m (1mm). Therefore, the difference is negligible considering the metric requirements to determine severity for this distress type. For the shape parameter, the value is less than 1 for all models, which signifies that the majority of the values within the distribution will largely occur early in the plot which indicates that a small measured difference is the likely outcome for a random point on the model. Considering this and the values of the scale parameters, it can also be inferred that the techniques have been validated for the range of mobile phones for this distress type as well.

**Table 5. Weibull parameters observed from each model comparison for the Pothole**

| | **Weibull parameters** | |
|---|---|---|
| **Phone** | **Shape (a)** | **Scale (b)** |
| Huawei P20 Pro | 0.735903 | 0.000138 |
| Samsung Galaxy s9 | 0.557118 | 0.000495 |
| iPhone XR | 0.853322 | 0.000102 |
| Google Pixel 2XL | 0.739198 | 0.000262 |
| Xiaomi Mi A1 | 0.684449 | 0.000593 |

## 8. CONCLUSIONS

The presented study was aimed at establishing the accuracy and reliability of using different mobile phones for data collection to carry out Structure-from-Motion 3D modelling techniques for the purpose of reconstructing and analysing pavement distresses. Once validated, this would be a cheap data acquisition pipeline as it utilizes mobile phones already typically owned by the average person.

To achieve this objective, five different mobile phones were used to reconstruct pavement distress image datasets from distresses occurring in an urban setting. Two specific distress types were chosen, a cracked section and a pothole, as these represent common distresses which are encountered in urban road networks and require measurement and analysis.

Imagery from each mobile phone was used to generate 3D models of the pavement distresses and these models were then analysed both from a visual and metric viewpoint.

From the results of the models of each distress type, it was shown that the models had differences in appearance and colour but with respect to a metric evaluation, the differences are negligible. This was shown through statistical analyses on each model considering a Weibull distribution which highlighted that the differences in the models were negligible in the context of evaluating the severity of pavement distresses. Therefore, this indicates that the techniques can be replicable in real-world scenarios with varying mobile phones validating the replicability of these modelling techniques in a real-world scenario.

Furthermore, given the advances of the phone industry, the available cameras on phones will also only become more advanced and therefore future models can achieve even higher resolutions. It also should be noted that for each of the phones tested, there are currently newer available models with better camera specifications, which would produce even greater results. Further work on this area will be needed for the consideration of more distress types.

Within the study, each 3D distress model, produced by the mobile phone imagery, was able to produce a model that could quantitatively measure and classify the distress based on the requirements of industry standards. Therefore the process can be further integrated within mobile applications to carry out the 3D reconstruction of the distress in real-time and be used for a quick reference guide for a road practitioner for a specific distress on a road network. This also removes subjectivity in the process and provides a cheaper alternative for procuring road condition data, which is necessary for an effective Pavement Management System. This, therefore, takes another step towards low-cost automation of pavement distress surveys.

## ACKNOWLEDGEMENTS

The research presented in this paper was carried out as part of the H2020-MSCA-ETN-2016. This project has received funding from the European Union's H2020 Programme for research, technological development and demonstration under grant agreement number 721493.

## REFERENCES

[1] International Road Federation (IRF), IRF World Road Statistics 2018 (Data 2011 -2016), Brussels, 2018.

[2] T.C. Mbara, M. Nyarirangwe, T. Mukwashi, Challenges of raising road maintenance funds in developing countries: An analysis of road tolling in Zimbabwe, J. Transp. Supply Chain Manag. 4 (2012) 151–175. doi:https://doi.org/10.4102/jtscm.v4i1.66.
[3] D. Peterson, National Cooperative Highway Research Program Synthesis of Highway Practice Pavement Management Practices. No. 135., Transportation Research Board, Washington, DC, 1987. http://onlinepubs.trb.org/Onlinepubs/nchrp/nchrp_syn_135.pdf.
[4] S.M. Bazlamit, H.S. Ahmad, T.I. Al-Suleiman, Pavement Maintenance Applications Using Geographic Information Systems, in: Procedia Eng., 2017: pp. 83–90. doi:10.1016/j.proeng.2017.03.123.
[5] S.C. Radopoulou, I. Brilakis, Improving Road Asset Condition Monitoring, Transp. Res. Procedia. 14 (2016) 3004–3012. doi:10.1016/j.trpro.2016.05.436.
[6] T.B.J. Coenen, A. Golroo, A review on automated pavement distress detection methods, Cogent Eng. 4 (2017) 1–23. doi:10.1080/23311916.2017.1374822.
[7] E. M. Mikhail, J. S. Bethel, C. Mcglone, Introduction to Modern Photogrammetry, New York, 2001.
[8] L. Inzerillo, G. Di Mino, R. Roberts, Image-based 3D reconstruction using traditional and UAV datasets for analysis of road pavement distress, Autom. Constr. 96 (2018). doi:10.1016/j.autcon.2018.10.010.
[9] M. Hullin, M. Stamminger, T. Weinkauf, V. Garro, G. Pintore, F. Ganovelli, E. Gobbetti, R. Scopigno, Fast Metric Acquisition with Mobile Devices, Vision, Model. Vis. (2016). doi:10.2312/vmv.20161339.
[10] W. Hauser, B. Neveu, J.-B. Jourdain, C. Viard, F. Guichard, Image quality benchmark of computational bokeh, Electron. Imaging. 2018 (2018) 340-1-340–10. doi:10.2352/issn.2470-1173.2018.12.iqsp-340.
[11] G. Loprencipe, A. Pantuso, A Specified Procedure for Distress Identification and Assessment for Urban Road Surfaces Based on PCI, Coatings. 7 (2017) 65. doi:10.3390/coatings7050065.
[12] K.C.P. Wang, W. Gong, Automated pavement distress survey: a review and a new direction, in: Pavement Eval. Conf., Roanoke, 2002: pp. 21–25. http://pms.nevadadot.com/2002presentations/43.Pdf.
[13] O.C. Puan, M. Mustaffar, T.-C. Ling, Automated Pavement Imaging Program (APIP) for Pavement Cracks Classification and Quantification, Malaysian J. Civ. Eng. (2007). http://eprints.utm.my/id/eprint/7828/1/LingTungChai2007_Automated_pavement_imaging_program_%28APIP%29.pdf.
[14] A. Elaksher, C. Zhang, 3D Reconstruction from UAV-acquired Imagery for Road Surface Distress Assessment, in: 31st Asian Conf. Remote Sens., 2010. http://www.a-a-r-s.org/acrs/administrator/components/com_jresearch/files/publications/TS12-2.pdf.
[15] K.C.P. Wang, Elements of automated survey of pavements and a 3D methodology, J. Mod. Transp. 19 (2011) 51–57. doi:10.1007/bf03325740.
[16] C. Zhang, A. Elaksher, 3D Reconstruction from UAV-acquired Imagery for Road Surface Distress Assessment, Aars.Org. (2009) 2–7. http://www.a-a-r-s.org/acrs/proceeding/ACRS2010/Papers/Oral Presentation/TS12-2.pdf.
[17] S.I. Sarsam, A.M. Ali, Assessing Pavement Surface Macrotexture Using Sand Patch Test and Close Range Photogrammetric Approaches, Int. J. Mater. Chem. Physics, Public Sci. Fram. Am. Inst. Sci. 1 (2015) 124–131.
[18] G. Caroti, I. Martínez-Espejo Zaragoza, A. Piemonte, Accuracy assessment in structure from motion 3D reconstruction from UAV-born images: The influence of the data processing methods, in: Int. Arch. Photogramm. Remote Sens. Spat. Inf. Sci. - ISPRS Arch., 2015. doi:10.5194/isprsarchives-XL-1-W4-103-2015.
[19] M.J. Westoby, J. Brasington, N.F. Glasser, M.J. Hambrey, J.M. Reynolds, “Structure-from-Motion” photogrammetry: A low-cost, effective tool for geoscience applications, Geomorphology. (2012). doi:10.1016/j.geomorph.2012.08.021.
[20] N. Snavely, S.M. Seitz, R. Szeliski, Modeling the world from Internet photo collections, Int. J. Comput. Vis. 80 (2008) 189–210. doi:10.1007/s11263-007-0107-3.
[21] C. Santagati, L. Inzerillo, F. Di Paola, Image-Based Modeling Techniques for Architectural Heritage 3D Digitalization: Limits and Potentialities, ISPRS - Int. Arch. Photogramm. Remote Sens. Spat. Inf. Sci. XL-5/W2 (2013) 555–560. doi:10.5194/isprsarchives-XL-5-W2-555-2013.
[22] F. Remondino, E. Nocerino, I. Toschi, F. Menna, A critical review of automated photogrammetric processing of large datasets, Int. Arch. Photogramm. Remote Sens. Spat. Inf. Sci. - ISPRS Arch. 42 (2017) 591–599. doi:10.5194/isprs-archives-XLII-2-W5-591-2017.
[23] J. Höhle, Oblique Aerial Images and Their Use in Cultural Heritage Documentation, ISPRS - Int. Arch. Photogramm. Remote Sens. Spat. Inf. Sci. XL-5/W2 (2013) 349–354. doi:10.5194/isprsarchives-xl-5-w2-349-2013.
[24] American Society for Testing and Materials. (ASTM), ASTM D 6433 -18 Standard Practice for Roads and Parking Lots Pavement Condition Index Surveys, West Conshohocken, 2018. doi:10.1520/D6433-18.
[25] Z.J. Arrospide E, Bikandi I, García I, Durana G, Aldabaldetreku G, Mechanical properties of polymer-optical fibres, in: B. Christian-Alexander, T. Gries, M. Beckers (Eds.), Polym. Opt. Fibres, Woodhead Publishing, 2017: pp. 201–216. doi:https://doi.org/10.1016/C2014-0-00562-X.
[26] D. Panagiotidis, P. Surový, K. Kuželka, Accuracy of Structure from Motion models in comparison with terrestrial laser scanner for the analysis of DBH and height influence on error behaviour, J. For. Sci. 62 (2016) 357–365. doi:10.17221/92/2015-JFS.